

## Isospin symmetry in the odd-odd mirror nuclei $^{44}\text{V}/^{44}\text{Sc}$

M. J. Taylor,<sup>1,\*</sup> M. A. Bentley,<sup>1</sup> J. R. Brown,<sup>1</sup> P. E. Kent,<sup>1</sup> R. Wadsworth,<sup>1</sup> C. J. Lister,<sup>2</sup> D. Seweryniak,<sup>2</sup> M. P. Carpenter,<sup>2</sup> R. V. F. Janssens,<sup>2</sup> S. Zhu,<sup>2</sup> T. Lauritsen,<sup>2</sup> L.-L. Andersson,<sup>3,†</sup> E. K. Johansson,<sup>3</sup> P. E. Garrett,<sup>4</sup> K. L. Green,<sup>4</sup> G. A. Demand,<sup>4</sup> and S. M. Lenzi<sup>5</sup>

<sup>1</sup>*Department of Physics, University of York, Heslington, York, YO10 5DD, United Kingdom*

<sup>2</sup>*Physics Division, Argonne National Laboratory, Argonne, Chicago, Illinois 60439, USA*

<sup>3</sup>*Department of Physics, Lund University, S-22100 Lund, Sweden*

<sup>4</sup>*Department of Physics, University of Guelph, Guelph, Ontario N1G2W1, Canada*

<sup>5</sup>*Dipartimento di Fisica dell'Università and INFN, Sezione di Padova, I-35131 Padova, Italy*

(Received 4 November 2011; published 19 December 2011)

Excited states in the  $N = Z - 2$  nucleus  $^{44}\text{V}$  have been observed for the first time. The states have been identified through particle- $\gamma$ - $\gamma$  coincidence relationships and comparison with analog states in the mirror nucleus  $^{44}\text{Sc}$ . Mirror energy differences have been extracted and compared to state-of-the-art shell-model calculations which include charge-symmetry-breaking forces. Observed decay pattern asymmetries between the mirror pair are discussed in terms of core excitations, electromagnetic spin-orbit effects and isospin mixing.

DOI: [10.1103/PhysRevC.84.064319](https://doi.org/10.1103/PhysRevC.84.064319)

PACS number(s): 21.10.Sf, 21.60.Cs, 23.20.Lv, 29.30.Kv

### I. INTRODUCTION

Symmetries play a key role in describing the properties of many-body quantum systems such as the atomic nucleus. If the strong nucleon-nucleon interaction is assumed to be both charge independent and charge symmetric, neglecting electromagnetic effects, symmetries between nuclei under the exchange of protons and neutrons (mirror nuclei) should arise. Nucleon-nucleon scattering measurements have shown that a slight charge asymmetry and charge dependence exists for free nucleon-nucleon interactions [1] and the degree to which these symmetries are broken for effective nucleon-nucleon interactions in the nuclear medium is still an open question. Indeed, Nolen and Schiffer [2] showed that, in spite of our in-depth understanding of the Coulomb force, the experimental binding energy difference between mirror nuclei cannot be reproduced theoretically.

The isospin formalism was developed to help describe such nucleon-exchange symmetries. Once this is combined with a reliable quantitative understanding of isospin-symmetry breaking phenomena (of Coulomb or non-Coulomb origin) this provides for an extremely effective framework for describing mirror energy differences (MEDs) between isobaric analog states (IAS). Measured MEDs in lower  $fp$ -shell nuclei, in conjunction with state-of-the-art shell-model calculations, have provided a plethora of nuclear structure information and have been the topic of extensive study in recent years (see [3] and references therein). Of particular interest was an observed anomaly in the isovector two-body matrix elements required to form a complete description of the observed spectra. This was in addition to the Coulomb matrix element for  $f_{7/2}$  protons

coupling to  $J = 2$ , for which an explanation has not yet been established. The majority of the experimental data that exist on MEDs in this region are for  $T = 1/2$  mirror pairs [4–14] or even-even  $T = 1$  mirrors and members of  $T = 1$  isobaric triplets [15–21]. Measurements have recently been extended to  $T = 3/2$  and  $T = 2$  analog nuclei [22,23].

No detailed MED data existed for odd-odd  $T_z = \pm 1$  mirror pairs until our recent study of the  $N = Z - 2$  nucleus  $^{48}\text{Mn}$  [21]. The measured yrast band MEDs for the  $^{48}\text{Mn}/^{48}\text{V}$  pair showed some unexpected phenomena. First, the MEDs were all below 40 keV (up to  $J^\pi = 13^+$ ) and the usual large differences ( $\sim 100$  keV) associated with angular momentum recoupling were absent. This was attributed to the fact that the Coulomb multipole effects would be small as the two nuclei (being mid-shell) have the same number of proton particles and holes. Second, a gradual rise in the MED was observed toward the band termination (albeit with a sudden dip at  $J^\pi = 8^+$ ). This trend was attributed to a reduction in the radius due to decreasing admixtures of the  $p_{3/2}$  orbital with increasing spin. We could not, however, find a physical interpretation for the sudden dip in the MED at  $J^\pi = 8^+$ , although it was reproduced perfectly in the model calculation. In order to shed light on the observed phenomena in  $^{48}\text{Mn}$  and to further test shell-model calculations in the lower half of the  $fp$  shell, it was important to study another odd-odd  $T_z = \pm 1$  mirror pair.

### II. EXPERIMENTAL TECHNIQUE

A constraint on the choice of reaction was the formation of an odd-odd  $N = Z$  compound nucleus in order to populate excited states in both of the mirror nuclei. A beam of  $^{36}\text{Ar}$  was accelerated to 95 MeV by the ATLAS facility at Argonne National Laboratory. The beam nuclei impinged on a  $0.25 \text{ mg/cm}^2$   $^{10}\text{B}$  target to produce  $^{46}\text{V}$  as a compound nucleus. Excited states were populated in the nuclei of interest,  $^{44}\text{V}$  and  $^{44}\text{Sc}$ , via the two-neutron (with estimated cross section  $\sigma = 0.7$  mb) and two-proton (with estimated  $\sigma = 123$  mb)

\*Present address: Department of Physics, and Astronomy, University of Manchester, Manchester, M13 9PL, UK; [m.j.taylor@manchester.ac.uk](mailto:m.j.taylor@manchester.ac.uk)

†Present address: Gesellschaft für Schwerionenforschung (GSI), Planckstrasse 1, D-64291 Darmstadt, Germany.

evaporation channels, respectively. The recoiling  $^{44}\text{V}$  and  $^{44}\text{Sc}$  nuclei were selected using the fragment mass analyzer (FMA) in conjunction with micro-channel plate (MCP) and gas ionization chamber (IC) detectors. Prompt  $\gamma$  rays were measured by the Gammasphere Ge detector array at the target position. In order to limit the count rate in the focal plane ionization chamber, slits were used to restrict nuclei with mass-to-charge ratios ( $A/Q$ ) other than  $\approx 3$ . This ratio was chosen to allow the  $^{44}\text{V}$  nuclei in charge state  $15^+$  (the majority) through to the focal plane. As the boron target suffered some oxidation, other reaction products with  $A/Q \approx 3$ , for example,  $^{16}\text{O}(^{36}\text{Ar},\alpha p)^{47}\text{V}$  nuclei with  $16^+$  charge states, were also transmitted to the focal plane. The data acquisition system recorded events consisting of either five or more  $\gamma$  rays detected in Gammasphere or any  $\gamma$  rays in coincidence with a MCP signal. The focal plane IC was electrically segmented to allow energy loss as well as total energy measurements. The IC pressure was adjusted to maximize the collection efficiency for vanadium nuclei. The segmentation of the IC allowed recoil  $Z$  identification via  $\Delta E$ - $E$  calorimetry. As different masses (in the same charge state) are distributed differently across the focal plane, the channel plate detector was used to further select the  $A = 44$  nuclei of interest.

To allow clean isotopic identification the recorded ion energy ( $E$  as recorded by the ion chamber) and time of flight ( $t$  as recorded between Gammasphere and the IC) were used. For a given flight path the mass of a particular ion is proportional to  $Et^2$  and therefore this quantity can be used to discriminate the  $\Delta A \approx 3$  charge-state ambiguities. The technique is detailed in Ref. [24] so only the results of the analysis will be discussed here.

### III. RESULTS

Figure 1(a) presents all prompt  $\gamma$  rays in coincidence with  $Z = 23$  ions entering the MCP and gas IC detectors. Contamination peaks resulting from  $A/Q$  ambiguities ( $^{47}\text{V}$ ), IC distribution overlaps ( $^{44}\text{Ti}$ ) and random correlations with large cross-section reaction products ( $^{44}\text{Sc}$  and  $^{44}\text{Ti}$ ) can be seen. Figure 2 shows the  $Et^2$  distributions for  $^{44}\text{V}$  and  $^{47}\text{V}$  from correlations with the 714 and 259 keV transitions, respectively. Two distributions are evident, showing a distinct separation for  $A = 44$  and  $A = 47$  recoils. By imposing an  $Et^2$  condition, with an appropriate background subtraction, a marked improvement in the cleanliness of the associated  $\gamma$  spectra was observed. Figure 1(b) has an  $A = 44$   $Et^2$  condition applied which eliminates all of the  $^{47}\text{V}$  contamination apart from two low-energy transitions at 58 and 87 keV that still remain due to poor detector timing characteristics at these energies. Figure 1(c) shows the same spectrum as that in Fig. 1(b) but with  $Z = 22$  and random correlations subtracted. A similar analysis was performed for  $^{44}\text{Sc}$  and the result is displayed in Fig. 3 along with that of its mirror  $^{44}\text{V}$  for comparison. A large degree of symmetry above  $\sim 500$  keV can be seen in the spectra shown in Fig. 3; however, a clear asymmetry exists at lower energies. Using Ref. [25] and mirror symmetry arguments as guidance, level schemes for  $^{44}\text{V}$  and  $^{44}\text{Sc}$  were deduced from recoil correlated  $\gamma$ - $\gamma$  coincidence data. Figure 4

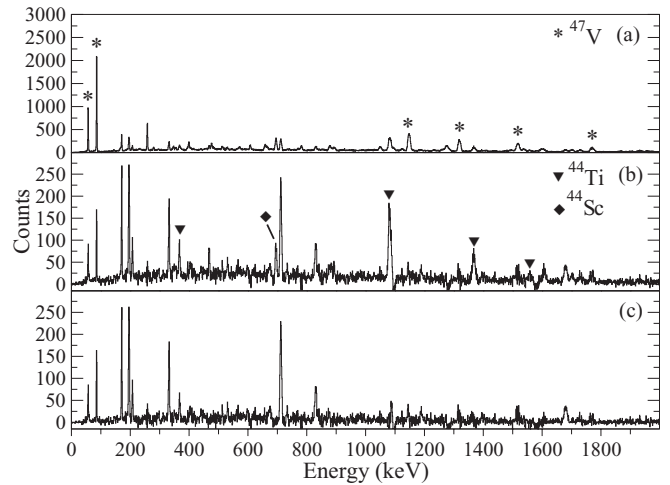


FIG. 1. (a)  $A/Q \approx 3$  and  $Z = 23$  gated particle- $\gamma$  spectrum.  $^{47}\text{V}$  transitions (starred) resulting from  $A/Q$  ambiguities are dominant. (b) The transitions from (a) but with a  $A = 44$   $Et^2$  condition. Neighboring  $Z = 22$  contaminant peaks (triangles) and random correlations (diamonds) can still be seen. (c)  $^{44}\text{V}$  spectrum produced by an  $A = 44$   $Et^2$  gate and with  $Z = 22$  and random coincidences subtracted.

provides the newly deduced scheme for  $^{44}\text{V}$  along with a partial level scheme for its mirror,  $^{44}\text{Sc}$ . Spins and parities for the excited states in  $^{44}\text{V}$  were deduced from mirror symmetry arguments and for states in  $^{44}\text{Sc}$  from Ref. [25]. The transition intensities were efficiency corrected and normalized to the 714 keV transition for  $^{44}\text{V}$  and to the 697 keV transition for  $^{44}\text{Sc}$ . The 67 keV  $1^-$  state in  $^{44}\text{Sc}$  has a half-life of 154 ns and is, therefore, absent in the prompt spectrum shown in Fig. 3. If we assume perfectly symmetric  $E1$  strengths, the analog state in  $^{44}\text{V}$  would have a half-life of around 6 ns. A 197 keV transition from the  $1^-$  state in  $^{44}\text{V}$  is present, albeit with reduced intensity, as the state can decay out of the focus of the Gammasphere array. Examination of

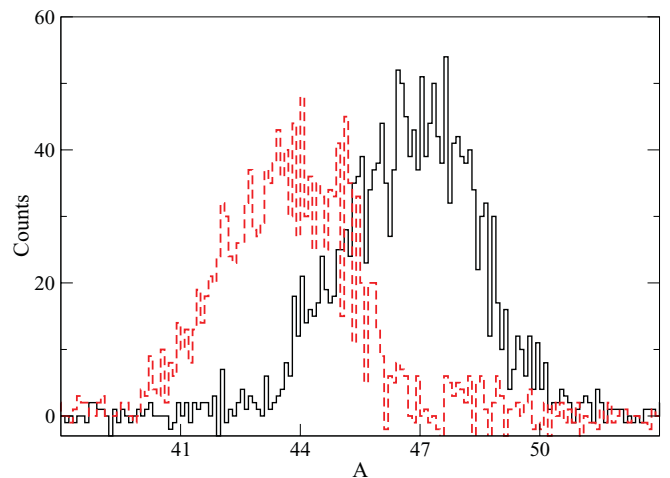


FIG. 2. (Color online)  $Et^2$  distributions corresponding to  $A = 44$  (dotted line) and  $A = 47$  (solid line) produced by selecting the 714 and 259 keV  $\gamma$  rays in  $^{44}\text{V}$  and  $^{47}\text{V}$ , respectively.

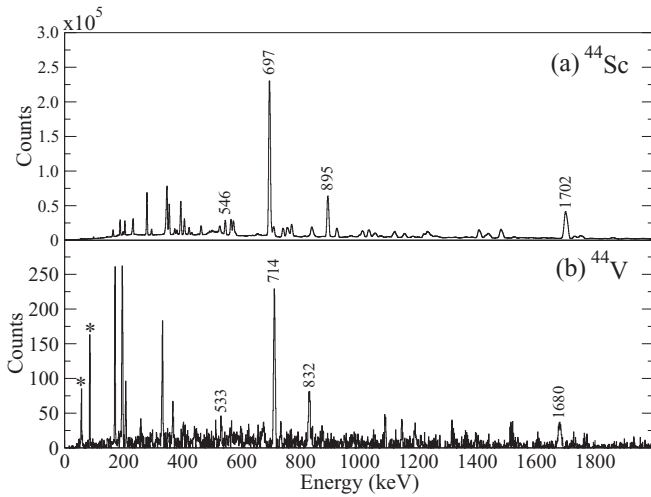


FIG. 3. (a)  $A = 44$   $E\tau^2$  gated and random-coincidences-subtracted  $^{44}\text{Sc}$  spectrum. (b)  $A = 44$   $E\tau^2$  gated,  $Z = 22$ , and random-coincidences-subtracted  $^{44}\text{V}$  spectrum. Starred (\*) transitions from  $^{47}\text{V}$  remain due to poor detector timing at low energies.

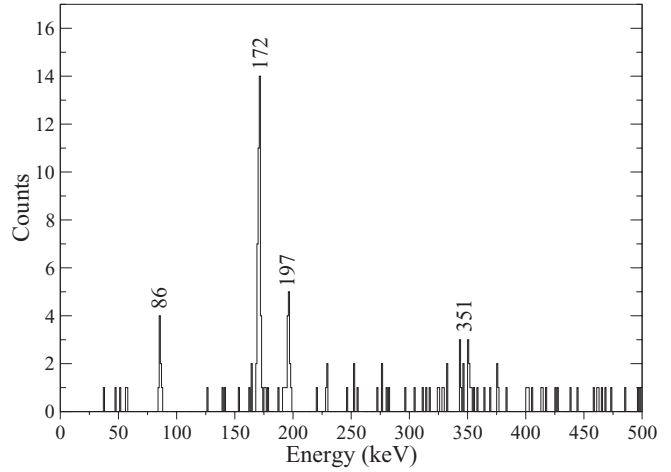


FIG. 5.  $^{44}\text{V}$   $\gamma$ -ray spectrum showing transitions in coincidence with 405 keV decays. The peak at 86 keV is a low-energy contaminant from  $^{47}\text{V}$  due to poor timing.

the feeding transitions shows there must be some 197 keV decay intensity missing with the efficiency-corrected value, as measured from Fig. 3, being 21(1)%. The missing intensity can be determined from the measured intensities of the 172 and 197 keV decays in coincidence with the 405 keV decay from the  $4^-$  state. Figure 5 presents a spectrum of 405 keV coincident  $\gamma$  rays. The 172 and 197 keV peak intensities show that 62% of the 197 keV decay intensity is lost due to the  $1^-$  state decaying downstream of the Gammasphere detectors. The intensity of the 197 keV decay in Fig. 4 has therefore been corrected for this missing intensity. Table I gives the measured relative intensities for all of the  $^{44}\text{V}$  transitions shown in Fig. 4.

Due to the isomeric nature of the  $6^+$  states, no depopulating decays were observed in this work. Also, for  $^{44}\text{V}$ , no decays populating the  $5^-$  state were observed and therefore no correlated  $5^- \rightarrow 6^+$  decays, which would determine the excitation energy of the  $6^+$  state, could be confirmed. Thus, it has not been possible with this data set to determine the excitation energy of the isomeric  $6^+$  state in  $^{44}\text{V}$ . For the purpose of the MED discussion, the MED for this state was deduced from the MED calculated in the framework of the shell model, the details of which are discussed below. Figure 4 only shows the mirrored transitions but the excitation energy of the  $6^+$  state in  $^{44}\text{Sc}$  was confirmed as that stated in Ref. [25] by the observation of transitions originating from the negative-parity structure feeding into the  $6^+$  and higher-lying yrast states.

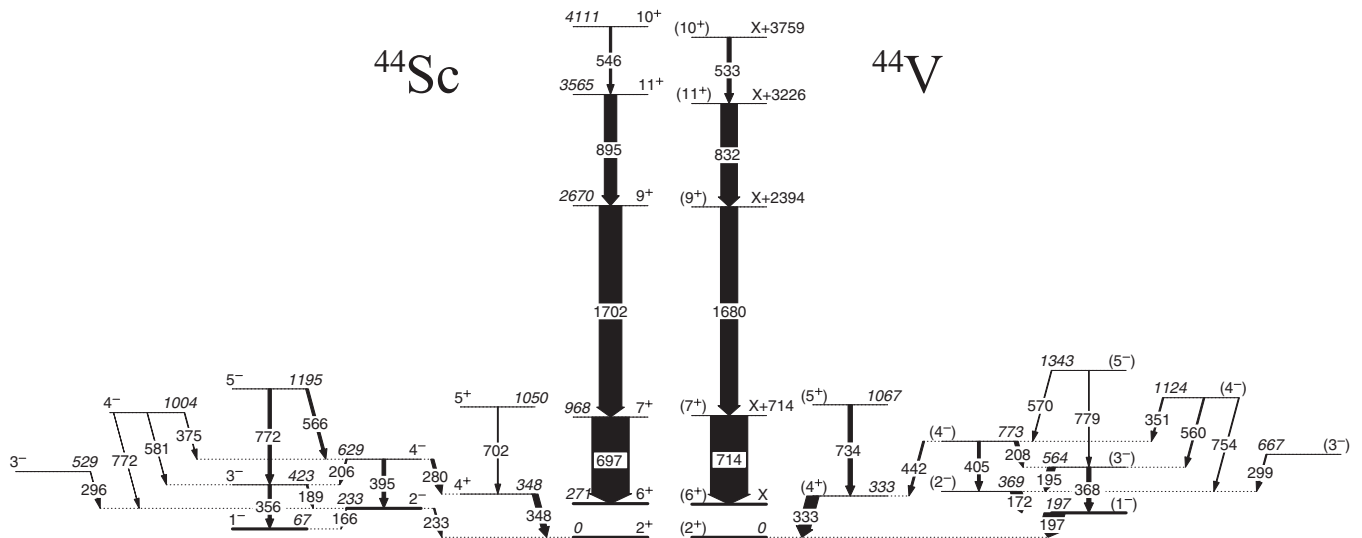


FIG. 4.  $^{44}\text{V}$  level scheme deduced using mirror symmetry arguments based on the  $^{44}\text{Sc}$  scheme from Ref. [25]. The corresponding partial scheme for  $^{44}\text{Sc}$  developed in this work is also shown for comparison. The intensity of the 197 keV decay out of the  $1^-$  state in  $^{44}\text{V}$  has been corrected for the loss of intensity due to its isomeric nature.

TABLE I. Energies and relative intensities of the newly observed  $^{44}\text{V}$   $\gamma$ -ray transitions normalized to the 714 keV decay. Spin and parity assignments for the initial ( $J_i^\pi$ ) and final ( $J_f^\pi$ ) states were deduced from mirror symmetry arguments. Depopulating state energies are also given.

$E_x$ (keV)	$E_\gamma$ (keV)	$I_{\text{rel}}$ (%)	$J_i^\pi$	$J_f^\pi$
979.9(5)	713.7(5)	100(4)	(7 <sup>+</sup> )	(6 <sup>+</sup> )
2659.9(17)	1680.0(16)	46(3)	(9 <sup>+</sup> )	(7 <sup>+</sup> )
3491.9(18)	832.0(7)	44(2)	(11 <sup>+</sup> )	(9 <sup>+</sup> )
4024.9(19)	533.0(7)	11(1)	(10 <sup>+</sup> )	(11 <sup>+</sup> )
332.6(4)	333.2(4)	32(2)	(4 <sup>+</sup> )	(2 <sup>+</sup> )
1067.0(13)	734.4(12)	11(1)	(5 <sup>+</sup> )	(4 <sup>+</sup> )
772.7(3)	442.2(8)	5(1)	(4 <sup>-</sup> )	(4 <sup>+</sup> )
	405.4(5)	7(1)	(4 <sup>-</sup> )	(2 <sup>-</sup> )
	208.4(2)	10(1)	(4 <sup>-</sup> )	(3 <sup>-</sup> )
564.1(2)	368.3(4)	11(1)	(3 <sup>-</sup> )	(1 <sup>-</sup> )
	194.8(2)	20(2)	(3 <sup>-</sup> )	(2 <sup>-</sup> )
368.9(1)	172.0(1)	30(1)	(2 <sup>-</sup> )	(1 <sup>-</sup> )
196.8(1)	196.8(1)	55(17) <sup>a</sup>	(1 <sup>-</sup> )	(2 <sup>+</sup> )
667.4(8)	298.6(8)	3(1)	(3 <sub>2</sub> <sup>-</sup> )	(2 <sup>-</sup> )
1123.9(9)	754.3(20)	2(1)	(4 <sub>2</sub> <sup>-</sup> )	(2 <sup>-</sup> )
	560.1(9)	4(1)	(4 <sub>2</sub> <sup>-</sup> )	(3 <sup>-</sup> )
	351.1(9)	3(1)	(4 <sub>2</sub> <sup>-</sup> )	(4 <sup>-</sup> )
1343.1(12)	779.1(12)	1(1)	(5 <sup>-</sup> )	(3 <sup>-</sup> )
	570.2(16)	2(1)	(5 <sup>-</sup> )	(4 <sup>-</sup> )

<sup>a</sup>Corrected for the missing downstream decay intensity (see text for details).

#### IV. DISCUSSION

Shell-model calculations have been performed to help interpret the experimentally observed MEDs as well as to place the isomeric 6<sup>+</sup> state in  $^{44}\text{V}$ . Calculations were performed using the code ANTOINE [26–28] and the KB3G interaction [29] which was modified to include known isospin-nonconserving effects. Following the method described in Ref. [30], the isospin-nonconserving terms computed were the following: the multipole Coulomb energy of the valence nucleons and the single-particle energy shifts due to Coulomb monopole effects (VCM), the monopole Coulomb energy associated with changes in radii as a function of spin (VCr) and the multipole interaction for two  $f_{7/2}$  protons coupled to  $J = 2$  (VB). The VB term is included to account for the anomalous  $J = 2$  matrix elements observed in similar studies for nuclei spanning the  $fp$  shell [3]. The calculations were performed over the full  $fp$  model space. Calculation of the negative-parity states would require the inclusion of two major shells ( $sd$  and  $fp$ ) for which no reliable interaction exists in this mass region; therefore, only calculations for the positive-parity states will be discussed.

Using the excitation energies of Fig. 4 experimental mirror energy differences were determined for the positive-parity states both feeding and bypassing the 6<sup>+</sup> isomer. Here, the MED between analog states is defined as  $E_x(^{44}\text{V}) - E_x(^{44}\text{Sc})$ . Theoretical MEDs were also determined from the shell-model-calculated state energies. Figure 6(a) compares the experimentally and theoretically determined MEDs. It is unfortunate that the excitation energy of the isomeric 6<sup>+</sup> state in  $^{44}\text{V}$  could not be determined experimentally in this work, thus removing the

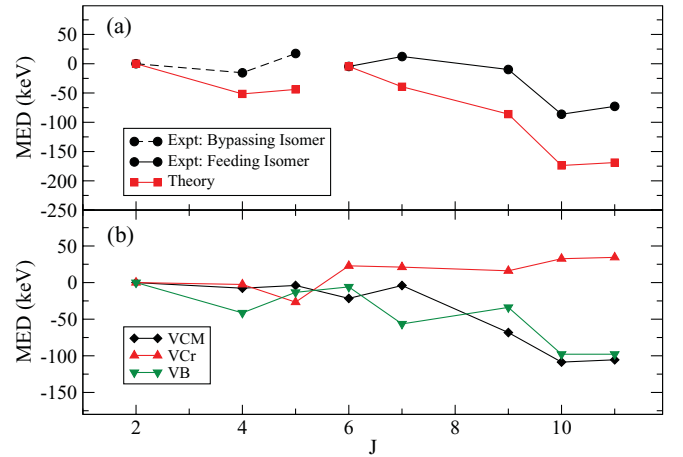


FIG. 6. (Color online) (a) Experimentally determined MEDs along with the theoretical MEDs calculated in the framework of the shell model. (b) The individual isospin-nonconserving contributions to the calculated MEDs shown in (a).

discontinuity in the MED curves. The MED value between the 6<sup>+</sup> states is, therefore, set as the calculated value of  $-5$  keV. Figure 6(b) shows the isospin-breaking contributions to the theoretical MEDs. At low spin, one might expect a relatively inactive MED, as spins up to 7<sup>+</sup> can be generated by the recoupling of the odd neutron and proton. This is largely borne out by the data, and the predicted multipole term is rather small also (which would reflect the recoupling of the protons in  $^{44}\text{V}$ ). Above this spin, the angular momentum must involve the recoupling of the protons in  $^{44}\text{V}$  (and neutrons in  $^{44}\text{Sc}$ ) with a resulting Coulomb effect. The theoretical prediction shows this, with the Coulomb multipole term exhibiting a gradual decrease at high spins caused by the reduction of the Coulomb energy in  $^{44}\text{V}$  as the protons recouple and reduce their spatial overlap (whereas, in  $^{44}\text{Sc}$ , the recoupling occurs for neutrons). The general form of the theoretical MED curve is matched by the data, but not the magnitude. It is interesting to note the contribution from the additional non-Coulomb isovector term associated with proton-proton  $J = 2$  couplings. In general terms, this effect (the  $J = 2$  anomaly) has as large a contribution as the Coulomb multipole term. The final term in the model prediction, the contribution from bulk Coulomb radial effects (VCr), is negligible, suggesting no change in the root-mean-square radius or deformation with increasing spin. This is not very surprising this low in the shell, where (i) the occupation of the  $p_{3/2}$  orbital (used in the model to “track” the changes in radius) is small and (ii) the proximity of the closed shell is likely to exclude significant deformation.

The difference in the magnitudes of the experimental and theoretical MEDs in Fig. 6(a) is of the order of 50 to 100 keV with the theoretical MEDs overestimating the measured values. This discrepancy could be significantly reduced by one of two actions. To obtain better agreement at high spin, one could set the experimental MED of the “floating” 6<sup>+</sup> state significantly lower (e.g.,  $-70$  keV or so). This seems unlikely, however, as there would then be a drop in the experimental MED of about 100 keV from the 5<sup>+</sup> to the 6<sup>+</sup> of which there is no hint in the calculation. The other possibility would be to

switch off the additional  $J = 2$  isovector term, which would give better agreement across the whole spin range. Again, the justification for this seems hard to establish, as the effect is seen to be important in almost every case observed so far in the shell. It has been demonstrated in Ref. [3] that a shell-model prescription, with all of the isospin-nonconserving effects included and parametrized consistently, is effective right across the shell. It therefore seems unjustified to remove one of the terms here. It is more likely that this discrepancy is, at least in part, due to the inadequacy of the shell model in the lower half of the  $fp$  shell, in that the valence space has not been extended to include  $2p$ - $2h$  excitations from the core. In this region, it has been shown that the shell model falls well short when describing the properties of the stable even- $A$  calcium isotopes without the inclusion of excitations from the presumed inert  $^{40}\text{Ca}$  core [31,32]. This is the most likely reason for this discrepancy. In the present calculation for  $A = 44$ , the multipole terms are large at high spin as, without any excitations from the  $sd$  shell, all the multipole Coulomb effects are restricted to  $^{44}\text{V}$  (as there is only one valence proton in  $^{44}\text{Sc}$ ). As soon as cross-shell excitations occur, which will happen at some level, this will no longer be the case, and the MED is likely to be smaller as a result. This is indeed what happens in the experimental data.

The experimental MED values for the negative-parity states were also determined and are compared in Fig. 7 with the MED values for the positive-parity states that are fed by the negative-parity structures. The negative-parity MEDs, unlike those for the positive-parity states, show a smooth trend, which is indicative of only small structural changes. This is consistent with the low-lying negative-parity states corresponding to a reasonably deformed prolate structure based on the cross-shell excitation of a  $d_{3/2}$  proton in  $^{44}\text{Sc}$  (or neutron in  $^{44}\text{V}$ ) into the  $f_{7/2}$  shell. For example, one would expect collective structures based on bandhead states in  $^{44}\text{Sc}$  ( $^{44}\text{V}$ ) created from coupling the  $[202]3/2$  proton-hole (neutron-hole) to the remaining unpaired neutron (proton) in the  $[321]3/2$   $f_{7/2}$  level. The slowly varying MED is consistent with the picture that the angular momentum is generated

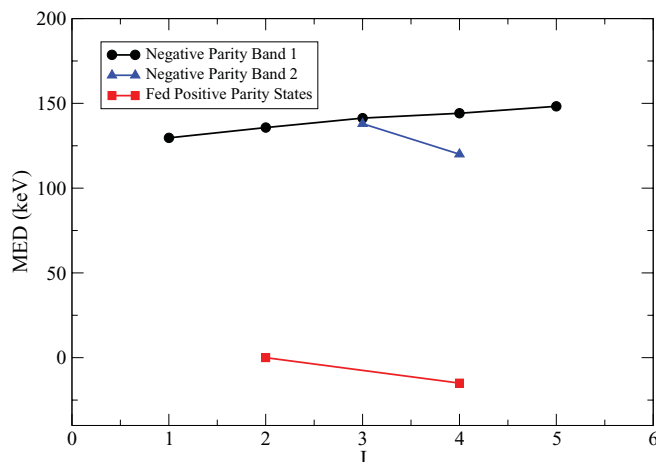


FIG. 7. (Color online) Mirror energy differences for the negative-parity states (circles and triangles) along with those of the positive-parity states (squares) that are fed by the negative-parity structures.

from a collective rotation rather than from any microscopic reconfigurations. Figure 7 also indicated that the MEDs for the negative-parity states lie  $\sim 140$  keV above the MEDs for the fed positive-parity states. This difference, at least in part, will arise from the single-particle electromagnetic shifts that affect the  $d_{3/2}$  and  $f_{7/2}$  orbits. These will become important for the MEDs for states described by excitations between these levels. In this case, the largest is the electromagnetic spin-orbit interaction [2,3], which contributes significantly to the MEDs for excitations between oppositely spin-orbit coupled orbitals, namely  $d_{3/2}(l-s)$  to  $f_{7/2}(l+s)$  excitations. This yields around 220 keV (calculated based on a charged sphere [2]) to the MED in this case, following the prescription laid out in Ref. [3] and assuming a pure proton (neutron) excitation in  $^{44}\text{Sc}$  ( $^{44}\text{V}$ ). The change in the single-particle Coulomb energy between these orbits, again calculated using the prescription in [3], is about  $-30$  keV, making a predicted shift of around 190 keV compared with the experimental 140 keV. A more refined calculation would need to include the bulk and single-particle effects of the change in deformation on the MED and use a more precise determination of the structure of the analog state concerned—which is beyond the scope of the current model. It is interesting to note that the MED for the second  $3_2^-$  states shown in Fig. 7 is of a similar magnitude, suggesting that these states are built upon a similar excitation.

In the absence of Coulomb interactions, by assuming the nuclear force is charge symmetric and charge independent, the level schemes for  $^{44}\text{V}$  and  $^{44}\text{Sc}$  should display a high degree of symmetry, not only in the energies of the states but in the feeding and decay patterns. Closer inspection of Fig. 4 shows that the low-lying transitions (redrawn schematically in Fig. 8) in the negative-parity structures exhibit a broken symmetry in this regard. No  $2^- \rightarrow 2^+$  decays are observed in  $^{44}\text{V}$  (expected at 369 keV), whereas a significant transition (233 keV) is observed in  $^{44}\text{Sc}$  despite the isomeric nature of the  $2^-$  state ( $t_{1/2} = 6.1(2)$  ns [33]), which will cause some of the decay intensity to be lost. Instead, in  $^{44}\text{V}$ , most of the intensity is carried by the 172 keV  $2^- \rightarrow 1^-$  transition, and the decay intensity out of the negative-parity structure therefore occurs at lower spins than in  $^{44}\text{Sc}$ . An upper limit on the intensity for the missing  $2^- \rightarrow 2^+$  transition can be obtained from Fig. 5. This figure shows a 405 keV transition coincidence spectrum and should contain the parity-changing

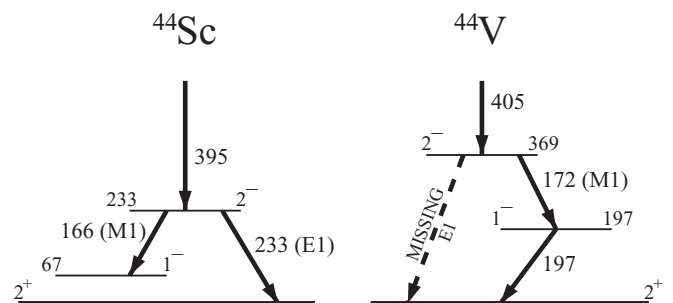


FIG. 8. A schematic low-energy level scheme, showing the  $\gamma$  rays observed in this work, to aid with the discussion of the absent 369 keV  $E1$  transition in  $^{44}\text{V}$  (see text for details).

369 keV decay out of the  $2^-$  state, if it exists, as well as the 172 keV parity-conserving transition. For the analog state in  $^{44}\text{Sc}$ , the parity-changing 233 keV transition is twice as strong as the parity-conserving 166 keV transition. It was estimated from Fig. 5 that a 369 keV transition of half the intensity of the 351 keV decay would be visible, and therefore this level of intensity forms an upper limit. Using the ratio of measured intensities for the 172 and 351 keV peaks in Fig. 5 the branching ratio of the parity-conserving to non-parity-conserving decays from the  $2^-$  state in  $^{44}\text{V}$  was determined to be  $>5:1$ . The corresponding ratio in  $^{44}\text{Sc}$  is 1:2, at least 10 times less than that measured in  $^{44}\text{V}$ ; moreover, the published data on the  $2^-$  state in  $^{44}\text{Sc}$  [33] shows that the  $M2$  component of the 166 keV  $\gamma$  ray is vanishingly small, as is the  $E2$  component of the 233 keV transition. Thus, it may be concluded that in both nuclei, the decay out of the  $2^-$  state is a competition between an  $E1$  and an  $M1$  transition. By using this information, and considering the different energies for the  $E1$  transitions, a comparison can be made between the  $B(E1)/B(M1)$  ratios for the decays from the two  $2^-$  states. Analysis shows that  $[B(E1)/B(M1)]_{\text{Sc}} > 40 [B(E1)/B(M1)]_{\text{V}}$ . This is a very large discrepancy and indicates an asymmetry in either the  $B(E1)$  or  $B(M1)$  reduced transition strengths between the mirror pair. There is no evidence in this region for any significant asymmetry in  $M1$  decay patterns between mirror nuclei; therefore the observed asymmetry must be due to the  $E1$  transitions. Despite the fact that isospin rules dictate that  $B(E1)$  should be identical in mirror nuclei, some cases of strong asymmetries in  $B(E1)$  strengths have been indicated by recent data, especially in the  $A = 35$  [34] and  $A = 31$  [35] mirror pairs, and the factor of 40 here does not seem out of line. A summary of the current situation regarding these asymmetries is given by Pattabiraman *et al.* [36] where factors ranging from 40 to 50 were also presented. For the nuclei presented in that work, the  $E1$  transitions were weak ( $10^{-6}$  or  $10^{-7}$  W.u.) and the analysis showed that, at least in the case of  $A = 35$ , such weak transition strengths can be strongly perturbed in the presence of moderate isospin mixing at the level of 1%, causing an asymmetry. A similar situation would seem to have arisen here.  $B(E1)$  for the 233 keV transition in

$^{44}\text{Sc}$  is known to be weak,  $4.7(3) \times 10^{-6}$  W.u.; if one assumes the  $M1$  strengths are the same, the much weaker  $B(E1)$  in  $^{44}\text{V}$  for the missing 369 keV transition must be of the order of, or weaker than,  $10^{-7}$  W.u.

## V. SUMMARY

Gamma-ray transitions have been observed, for the first time, in the  $T_z = -1$  nucleus  $^{44}\text{V}$ . Using  $\gamma$ - $\gamma$  coincidences and mirror symmetry arguments, a new level scheme for  $^{44}\text{V}$  has been proposed. Experimental mirror energy differences between analog states in the mirror pair have been determined and, for the positive-parity states, compared to those calculated by the shell model with the inclusion of isospin-nonconserving forces. The theoretical MED track the general trend of the data very well but overestimate the MED by around 50–100 keV. This discrepancy has been attributed to the exclusion of core excitations from the  $sd$  shell in the model. Indeed, an effective interaction in a model space that allows such excitations would be highly desirable. The MEDs for the negative-parity states show a smooth trend, in contrast to those of the positive-parity states, indicating only small structural changes. This trend has been attributed to particle-hole excitations from the  $sd$  shell and the energy difference between the negative-parity MEDs and the fed positive-parity MEDs is consistent with that expected from the electromagnetic spin-orbit interaction. The  $^{44}\text{Sc}/^{44}\text{V}$  level schemes have highlighted major asymmetries between the decay patterns, in particular the absence of a  $2^- \rightarrow 2^+$   $E1$  transition in  $^{44}\text{V}$ , which can be understood in terms of reduced  $E1$  strength arising from a small amount of isospin mixing.

## ACKNOWLEDGMENTS

The authors wish to thank the accelerator staff at the ATLAS facility. This work is supported by the US Department of Energy, Office of Nuclear Physics, under Contract No. DE-AC02-06CH11357.

- 
- [1] R. Machleidt and H. Muther, *Phys. Rev. C* **63**, 034005 (2001).  
 [2] J. A. Nolen and J. P. Schiffer, *Annu. Rev. Nucl. Sci.* **19**, 471 (1969).  
 [3] M. A. Bentley and S. M. Lenzi, *Prog. Part. Nucl. Phys.* **59**, 497 (2007).  
 [4] J. A. Cameron, M. A. Bentley, A. M. Bruce, R. A. Cunningham, W. Gelletly, H. G. Price, J. Simpson, D. D. Warner, and A. N. James, *Phys. Lett. B* **235**, 239 (1990).  
 [5] J. A. Cameron, M. A. Bentley, A. M. Bruce, R. A. Cunningham, W. Gelletly, H. G. Price, J. Simpson, D. D. Warner, and A. N. James, *Phys. Rev. C* **44**, 1882 (1991).  
 [6] J. A. Cameron, M. A. Bentley, A. M. Bruce, R. A. Cunningham, H. G. Price, J. Simpson, D. D. Warner, A. N. James, W. Gelletly, and P. V. Isacker, *Phys. Lett. B* **319**, 58 (1993).  
 [7] J. A. Cameron, M. A. Bentley, A. M. Bruce, R. A. Cunningham, W. Gelletly, H. G. Price, J. Simpson, D. D. Warner, and A. N. James, *Phys. Rev. C* **49**, 1347 (1994).  
 [8] C. D. O'Leary, M. A. Bentley, D. E. Appelbe, D. M. Cullen, S. Erturk, R. A. Bark, A. Maj, and T. Saitoh, *Phys. Rev. Lett.* **79**, 4349 (1997).  
 [9] D. Rudolph *et al.*, *Z. Phys. A* **358**, 379 (1997).  
 [10] M. A. Bentley, C. D. O'Leary, A. Poves, G. Martínez-Pinedo, D. E. Appelbe, R. A. Bark, D. M. Cullen, S. Erturk, and A. Maj, *Phys. Lett. B* **437**, 243 (1998).  
 [11] M. A. Bentley *et al.*, *Phys. Rev. C* **62**, 051303 (2000).  
 [12] J. Ekman *et al.*, *Eur. Phys. J. A* **9**, 13 (2000).  
 [13] S. J. Williams *et al.*, *Phys. Rev. C* **68**, 011301 (2003).  
 [14] M. A. Bentley *et al.*, *Phys. Rev. C* **73**, 024304 (2006).  
 [15] C. E. Svensson *et al.*, *Phys. Rev. C* **58**, R2621 (1998).  
 [16] S. M. Lenzi *et al.*, *Phys. Rev. C* **60**, 021303 (1999).  
 [17] C. D. O'Leary, M. A. Bentley, D. E. Appelbe, R. A. Bark, D. M. Cullen, S. Erturk, A. Maj, J. A. Sheikh, and D. D. Warner, *Phys. Lett. B* **459**, 73 (1999).  
 [18] P. E. Garrett *et al.*, *Phys. Rev. Lett.* **87**, 132502 (2001).

- [19] S. M. Lenzi *et al.*, *Phys. Rev. Lett.* **87**, 122501 (2001).
- [20] C. D. O’Leary *et al.*, *Phys. Lett. B* **525**, 49 (2002).
- [21] M. A. Bentley *et al.*, *Phys. Rev. Lett.* **97**, 132501 (2006).
- [22] J. R. Brown *et al.*, *Phys. Rev. C* **80**, 011306 (2009).
- [23] P. Doornenbal *et al.*, *Phys. Lett. B* **647**, 237 (2007).
- [24] S. J. Freeman *et al.*, *Phys. Rev. C* **69**, 064301 (2004).
- [25] M. Lach *et al.*, *Eur. Phys. J. A* **25**, 1 (2005).
- [26] E. Caurier, shell-model code ANTOINE, IReS, Strasbourg, 1989–2004.
- [27] E. Caurier and F. Nowacki, *Acta Phys. Pol. B* **30**, 705 (1999).
- [28] E. Caurier, G. Martínez-Pinedo, F. Nowacki, A. Poves, and A. P. Zuker, *Rev. Mod. Phys.* **77**, 427 (2005).
- [29] A. Poves, J. Sanchez-Solano, E. Caurier, and F. Nowacki, *Nucl. Phys. A* **694**, 157 (2001).
- [30] A. P. Zuker, S. M. Lenzi, G. Martínez-Pinedo, and A. Poves, *Phys. Rev. Lett.* **89**, 142502 (2002).
- [31] M. J. Taylor *et al.*, *Phys. Lett. B* **559**, 187 (2003).
- [32] M. J. Taylor *et al.*, *Phys. Lett. B* **605**, 265 (2005).
- [33] J. A. Cameron and B. Singh, *Nucl. Data Sheets* **88**, 299 (1999).
- [34] J. Ekman *et al.*, *Phys. Rev. Lett.* **92**, 132502 (2004).
- [35] D. G. Jenkins *et al.*, *Phys. Rev. C* **72**, 031303 (2005).
- [36] N. S. Pattabiraman *et al.*, *Phys. Rev. C* **78**, 024301 (2008).